

A WATERMARKING SCHEME FOR DIGITAL IMAGES USING MULTILEVEL WAVELET DECOMPOSITION

Muhammad Shafique Shaikh and Yasuhiko Dote

Department of Computer Science and Systems Engineering

Muroran Institute of Technology

27-1 Mizumoto Cho, Muroran

Japan

Tel.: 81-143-46-5475

Fax: 81-143-46-5499

email: rsmab@yahoo.com

ABSTRACT

A robust multilevel watermarking method based on multiresolution wavelet transformation is introduced. The coefficients of watermark are embedded into those of host image at different transformation level with a novel procedure. Watermark is extracted by inverse transformation at every level and by feeding the residual marked image to the subsequent level. Finally, the watermark is estimated by taking mean value of the watermarks obtained at every level. The introduced method is tested on six gray images with added Gaussian, salt and pepper, Speckle, and JPEG noises. The method is also examined with a color mpeg video. Signal to noise ratio with correlation coefficients are used as criteria for testing the method.

Keywords: *Copyright Protection, Watermarking, Digital Image, Wavelet Transformation*

1.0 INTRODUCTION

In the age of rapidly growing Internet technology and availability of multimedia computing facilities, the protection of intellectual property rights has become a vital issue. In particular it is true for image and video data. Conventionally, to identify the source a painting is signed by the artist, an identity card is stamped by a seal, and a paper money is embossed by a portrait [1].

In the academic literature, several techniques have been developed for watermarking. Detailed reviews are given in [2, 3, 4]. Current techniques for watermarking of images can be grouped into two classes: transform domain methods [5, 6, 7], which embed the data by modulating the transform domain coefficients, and spatial domain techniques [8, 9]. We utilise multilevel wavelet decomposition for our study and present a technique to embed the watermark in each of the resolution levels.

It is found in the literature that multi-resolution wavelet-based fusion algorithms are superior to other image merging techniques [7]. The localisation of the watermark at high resolution provides the ability to identify distinct regions of the watermarked image, which have undergone tampering, and global spreading of the watermark at low resolutions within the host makes it robust to large-scale signal distortions [10]. We described the watermark scheme based on multi-level wavelet transformation and test with gray scale images with additional Gaussian, salt and pepper, Speckle, and JPEG noises. The method is also examined with a color mpeg video with additive Gaussian, salt and pepper, and Speckle noises.

Section 2 describes our novel multilevel watermarking method. Similarity measure is presented in Section 3. We discuss our simulation results on gray scale images and color mpeg video in Sections 4 and 5 respectively and conclude our paper in Section 6.

2.0 NOVEL MULTILEVEL WATERMARKING METHOD

In our method we use binary watermark comprised of $N \times N$ arrays of ones and zeros. For simplicity, we adopt the notation scheme used in [6] with some modifications. It is assumed that the size of the watermark in relation to the host image is small. We use $f(m,n)$ to denote the host image and $w(p,q)$ the watermark; where m and n denote the image dimension and p and q represent the watermark size. A general view of watermarking method is shown in Fig. 1. The watermark embedding and retrieval method [11, 12] is described in the following subsections.

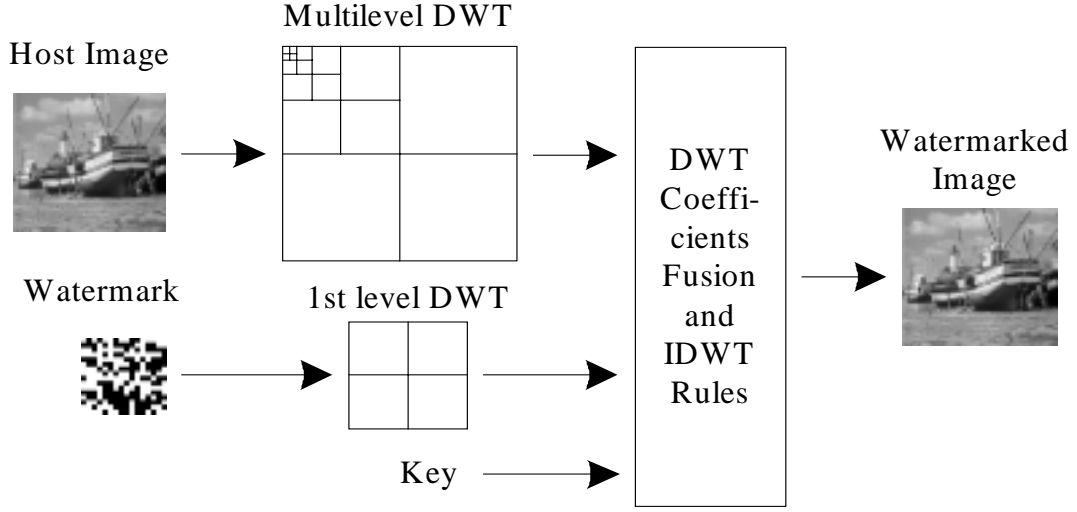


Fig. 1: Proposed watermarking method

2.1 Watermark Embedding

The presented watermark embedding scheme is comprised of following two steps.

Step I:

Both the host image and the watermark are transformed into the wavelet domain. The number of levels (L) of discrete wavelet transformation (DWT) depends on the size of the watermark. The DWT of the host image produces three detail images, *i.e.*, horizontal, vertical, and diagonal details at each resolution levels, and an approximation of the image at L th level. The detail coefficients of the host image and watermark are denoted by $f_{k,l}(m,n)$ and $w_{k,l}(p,q)$, respectively, where $k=1,2,3$ represent horizontal, vertical, and diagonal details, and $l=1,\dots,L$. We perform only first level DWT of the watermark.

Step II:

Let's denote the number of coefficients in k details of l level of DWT of the host image as $s_{k,l}$ and that of watermark as $t_{k,l}$. We randomly select $s_{k,l}$ using a secret for watermark embedding and denote it as $r_{k,l}(p,q)$. Therefore, for every level l :

1. Add the watermark coefficients $w_{k,l}(p,q)$ to the $f_{k,l}(m,n)$ at locations pointed at by $r_{k,l}(p,q)$.
2. Inverse transform and feed marked image to the next level of embedding.

We denote the watermarked image after L times of embedding as $\tilde{f}(m,n)$.

2.2 Watermark Extraction

Extraction of watermark is comprised of following two steps.

Step I:

The watermark is extracted from the possibly corrupted marked image by applying the inverse procedure at each resolution level. Let's denote the detail coefficients of $\tilde{f}(m,n)$ for every l level of wavelet decomposition as $\tilde{f}_{k,l}(m,n)$. We need host image and the secret key to generate $r_{k,l}(p,q)$ for extraction of the watermark.

Therefore, for every level l :

1. Subtract the host detail coefficients $f_{k,l}(m,n)$ from those of noisy marked image, $\tilde{f}_{k,l}(m,n)$, only from the locations pointed at by $r_{k,l}(p,q)$. Store the residual marked image for further processing in next step.
2. Inverse transform the extracted watermark coefficients and residual watermarked coefficients for 1st level and l level respectively. The extracted watermark is denoted by $\hat{w}_l(p,q)$. Feed the residual marked image to the next level of watermark extraction.

Step II:

Estimate the watermark by averaging the extracted watermarks $\hat{w}_l(p,q)$ and normalise it for binary values.

3.0 SIMILARITY MEASURE

In order to find out similarity between embedded and extracted watermarks first we observe the host and the marked images perceptually. We calculate correlation coefficients between them at different signal to noise ratio (SNR) values.

The correlation coefficient, ρ , used for similarity measurement, and SNR are defined as

$$\rho(w, \hat{w}) = \frac{\sum_{i=1}^N w_i \hat{w}_i}{\sqrt{\sum_{i=1}^N w_i^2} \sqrt{\sum_{i=1}^N \hat{w}_i^2}} \quad (1)$$

$$SNR(w, \hat{w}) = 10 \log_{10} \frac{\sum_{i=1}^N w_i^2}{\sum_{i=1}^N (w_i - \hat{w}_i)^2} \quad (2)$$

where N is the number of pixels in watermark, and w and \hat{w} are the original and extracted watermarks, respectively.

4.0 SIMULATION RESULTS AND DISCUSSION

For simulation of the presented watermarking method we chose six 256x256 gray intensity images, *i.e.* *bird*, *cameraman*, *fishingboat*, *goldhill*, *rice*, and *tyre*, and two 16x16 binary watermarks where one is randomly generated while the other has English text, ICLMIT, as shown in Fig. 2. Haar wavelet was used in our simulation. Selected level of DWT for host image is 5th while for the watermark it is first because the size of detail coefficients are same at these levels. The dimensions of transformed components of host image, *i.e.* $f_{k,l}(m,n)$ where $k=1,2,3$ denote horizontal, vertical, and diagonal, and $l=1, \dots, L$, and that of watermark, *i.e.* $w_{k,l}(p,q)$, are shown in Tables 1 and 2, respectively.

The decomposed watermark coefficients were embedded into those of the host image using Steps I to II of the presented watermark embedding method. The host and marked images using *random* and *text* watermarks are shown in Fig. 3. There is no perceptual distortion in these images it means that our scheme has satisfied the first criteria. Although perceptually we do not find any difference in the host and marked images but some degradation might have occurred in the process of watermark embedding. In order to find the degradation we calculated the peak signal to noise ratio (PSNR) between the host and marked images and compared our result with that of [13]. For this comparison we use the same formula that is used in [13], *i.e.*,

$$RMSE = \sqrt{\frac{1}{M * N} \sum_{i=1}^M \sum_{j=1}^N [\hat{f}(m,n) - f(m,n)]^2} \quad (3)$$

where (M, N) is the size of host image, f , and the watermarked image \hat{f} , and RMSE represents root-mean-square error. The related measure of PSNR (in dB) is computed using

$$PSNR = 20 \log_{10} \left[\frac{255}{RMSE} \right] \quad (4)$$

for the 8-bit (0-255) image.



(a) Random watermark (b) Text watermark

Fig. 2: Original *random* and *text* watermarks

Table 1: Wavelet decomposed host image components

Layer	Horizontal	Vertical	Diagonal
1	128 x 128	128 x 128	128 x 128
2	64 x 64	64 x 64	64 x 64
3	32 x 32	32 x 32	32 x 32
4	16 x 16	16 x 16	16 x 16
5	8 x 8	8 x 8	8 x 8

Table 2: Wavelet decomposed watermark components

l	Horizontal	Vertical	Diagonal
1	8 x 8	8 x 8	8 x 8

The PSNR values are calculated using a watermark scaling factor, α , for the range 0.1 to 1.0. Table 3 shows that our scheme gave better result as compare to that of [13]. Average improvement in PSNR is found as 633%.

For rest of the simulation we computed the SNR using Eq. (2) and did not use the scaling factor, α .

Table 3: Performance evaluation

α	PSNR [13] (dB)	PSNR (dB)	Improvement (%)
0.1	27.11	92.32	341
0.2	20.98	86.30	411
0.3	17.41	82.77	475
0.4	14.81	80.28	542
0.5	12.70	78.34	617
0.6	11.36	76.75	676
0.7	10.48	75.41	720
0.8	9.60	74.25	773
0.9	8.69	73.23	843
1.0	7.79	72.32	928

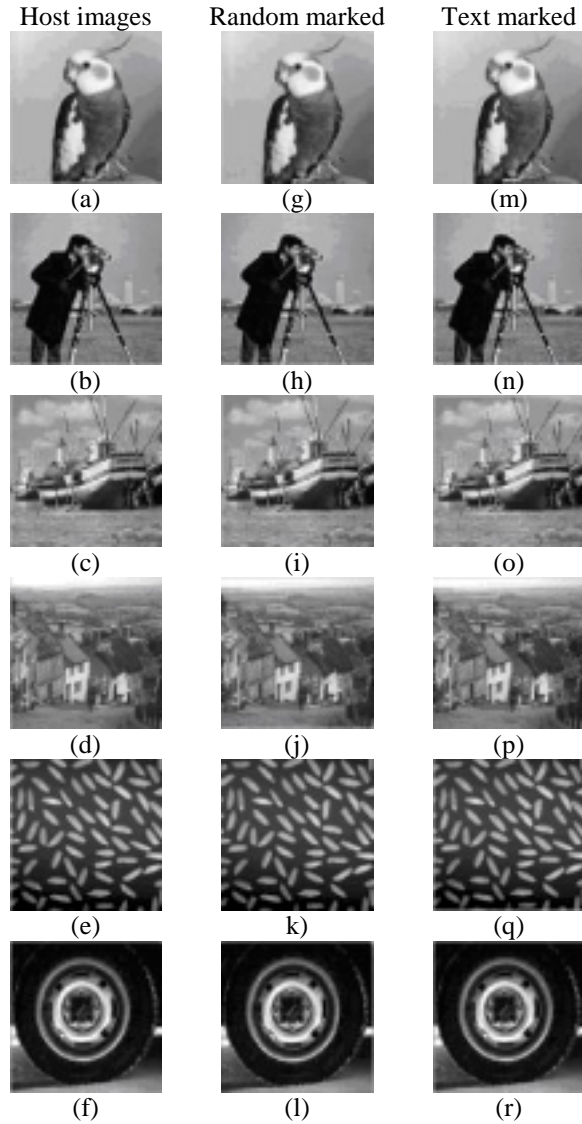


Fig. 3: Host and *random* and *text* watermarked images

To verify the robustness of the presented method the marked images were distorted by adding *Gaussian*, *salt & pepper*, and *Speckle* noises, and were subjected to lossy *joint photographic experts group* (JPEG) compression that is widely used for digital image storage and communication in Internet community. For our method we suppose that the correlation coefficient, ρ , of about 0.75 or above is an acceptable value. Acceptable value of ρ may vary from person to person.

4.1 Effect of Gaussian Noise

For adding the Gaussian noise to the marked images we fixed the mean at zero and changed the variance. We calculated correlation coefficients, ρ , for the extracted *random* and *text* watermarks at different SNR values as shown in Fig. 4 and Fig. 5, respectively. We notice that ρ remain above 0.96 in most of the cases and then reach the value 1 and maintains it for SNR 46.0 dB and above for all the images. The correlation coefficients are well above the set criteria. This means that our method sustained the degradation caused by the Gaussian noise of the given variance.

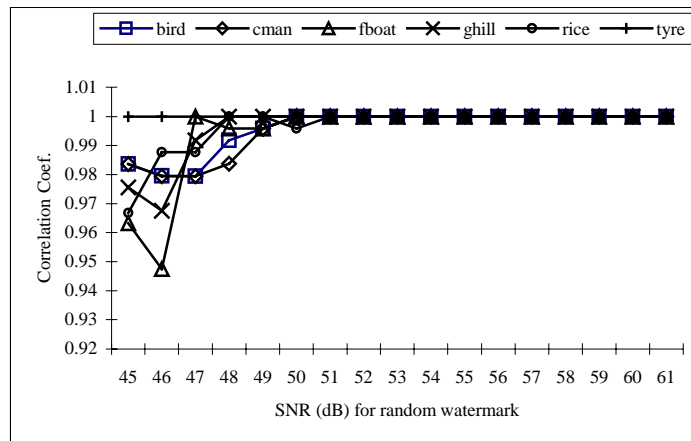


Fig. 4: Result for additive *Gaussian* noise using *random* watermark on six marked images

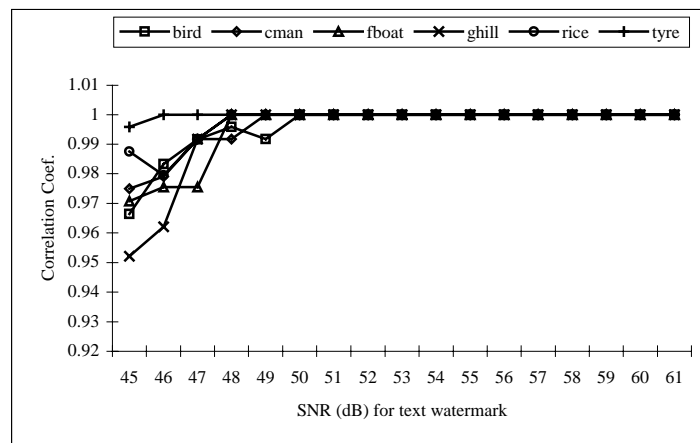


Fig. 5: Result for additive *Gaussian* noise using *text* watermark on six marked images

4.2 Effect of Salt and Pepper Noise

The random salt and pepper noise of various densities was added to the marked image. Fig. 6 and Fig. 7 show the correlation coefficient, ρ , patterns at different SNR values for the extracted *random* and *text* watermarks from all *salt and pepper* noised images. For the given range of noise the ρ started increasing from 0.5 and reached its maximum value 1 gradually. It crosses the desired criteria of 0.75 at about 24 dB SNR that is an acceptable value. Hence, the presented scheme sustained the degradation caused by *salt and pepper* noise of the given density.

4.3 Effect of Speckle Noise

Next the marked images were distorted by random Speckle noise of different density values. Fig. 8 and Fig. 9 show the correlation coefficients, ρ , patterns at different SNRs for the extracted watermarks from all *Speckle* noised marked images using *random* and *text* watermarks. The shapes of the correlation coefficient patterns are nearly the same in all cases. The correlation coefficient, ρ , increased gradually from 0.6 to 1 for SNR of 30 dB and above. It reached 0.75, the criteria, at about 35 dB SNR, which is an acceptable value.

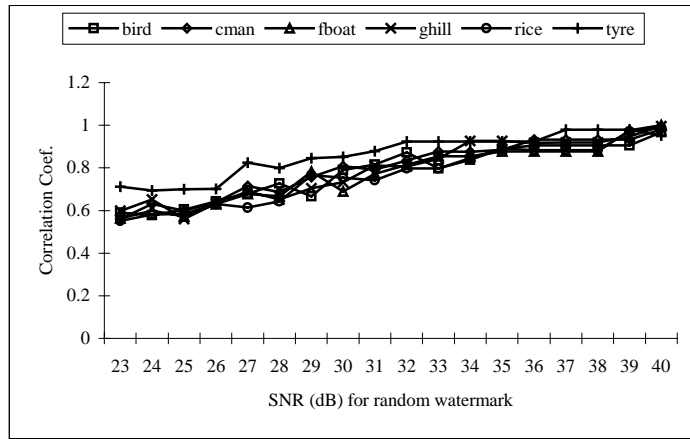


Fig. 6: Result for additive *salt and pepper* noise using *random* watermark on six marked images

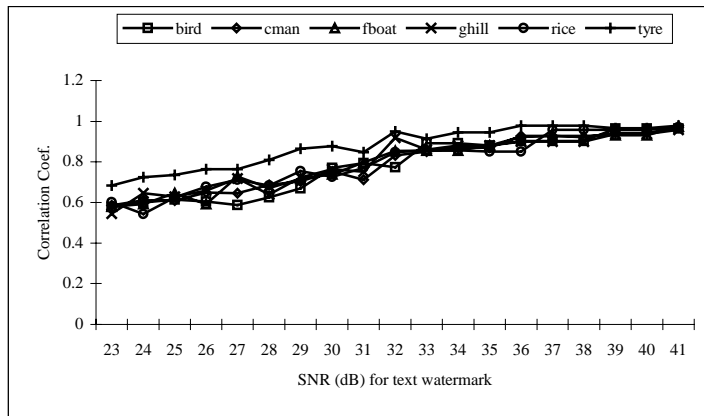


Fig. 7: Result for additive *salt and pepper* noise using *text* watermark on six marked images

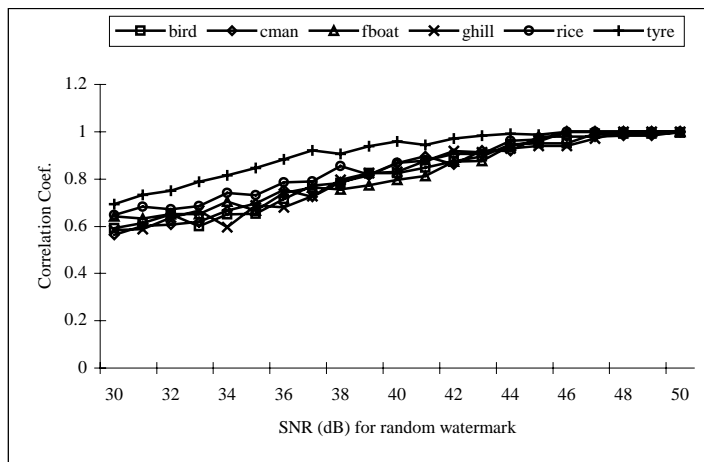


Fig. 8: Result for additive Speckle noise using *random* watermark on six marked images

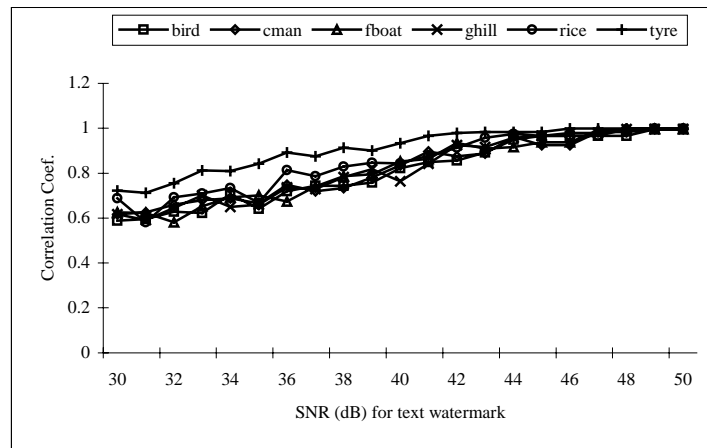


Fig. 9: Result for additive Speckle noise images using *text* watermark on six marked images

4.4 Effect of Lossy JPEG Compression

Lossy JPEG compression technology is commonly used in the Internet community for image storage and communication. We subjected the watermarked images to lossy JPEG compression to see the effect on extracted watermarks for quality factors from 0 to 100. The correlation coefficient, ρ , for all images, obtained at different SNR values for the extracted *random* and *text* watermarks for lossy JPEG compression are shown in Fig. 10 and Fig. 11, respectively. We observe that the correlation coefficient increases gradually from about 0.5 to 1. Quality factor of 75 is widely used in Internet community. We notice that ρ remain well near 1.0 in all cases for the quality factor 75 (i.e. at about SNR=8 dB) and above.

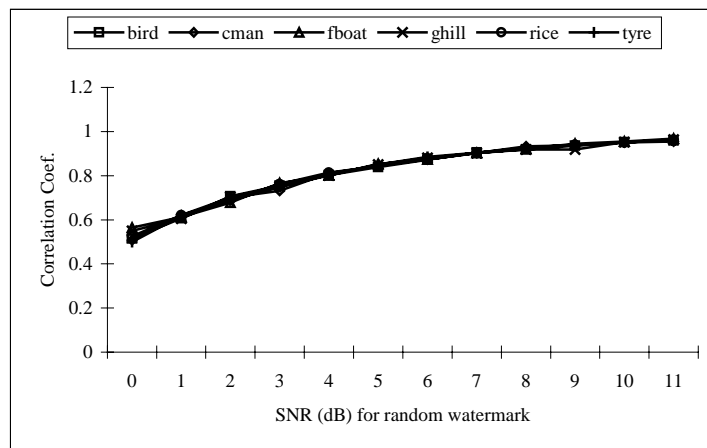


Fig. 10: Result for additive *JPEG* noise using *random* watermark on six marked images

5.0 WATERMARKING OF VIDEO

Just a few years ago, video was a form of creative expression intended only for tape, film, and television. However, now that broadband connections such as cable and digital subscriber line (DSL) are rising in popularity, we are seeing a dramatic increase in the use of video on Web sites and as attachments to E-mail.

Video has many commonly used file formats, and those file formats each come with a unique and sometimes complicated set of options, two of the most common file formats are audio video interleave (AVI) and moving picture experts group (MPG or MPEG).

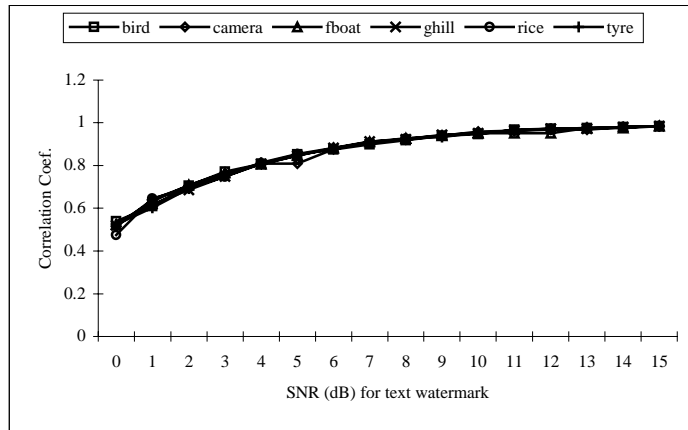


Fig. 11: Result for additive *JPEG* noise using *text* watermark on six marked images

MPEG-2 and MPEG-4 are newer, more flexible, and more powerful MPEG Media Type. The quality of MPEG-4 can be so good that it is used in digital versatile disk (DVD) and digital satellite television. In our study of watermarking we embed watermark into a MPEG-1 video.

Watermarking of video can be found in [14, 15]. We consider the *museum* video [15] stored in MPEG format. The video comprises of 30 frames. Before transforming the color frames into wavelet domain we converted the RGB image into YC_bC_r color scheme that is widely used for digital video. In this format, luminance information is stored as a single component (Y), and chrominance information is stored as two color-difference components (C_b and C_r). C_b represents the difference between the blue component and a reference value. C_r represents the difference between the red component and a reference value. The conversion formulae from RGB to YC_bC_r and vice versa are given in Eqs. 5 and 6, respectively. For transforming into wavelet domain and embedding of watermark we use only the luminance (Y) of the host image.

$$\begin{aligned}
 Y &= 0.299 R + 0.587 G + 0.114 B \\
 C_b &= -0.1687 R - 0.3313 G + 0.5 B + 128 \\
 C_r &= 0.5 R - 0.4187 G - 0.0813 B + 128
 \end{aligned}
 \tag{5}$$

$$\begin{aligned}
 R &= Y + 1.402 (C_r - 128) \\
 G &= Y - 0.34414 (C_b - 128) - 0.71414 (C_r - 128) \\
 B &= Y + 1.772 (C_b - 128)
 \end{aligned}
 \tag{6}$$

We chose a randomly generated binary watermark of size 16x16, as shown in Fig. 2(a). The size of each video frame is 240x352 so we selected the level of DWT up to four and chose level one for the watermark. The size of wavelet transformed components of host video frame and the watermark is given in Tables 4 and 5, respectively.

Table 4: Size of wavelet decomposed video frame components

Level	Horizontal	Vertical	Diagonal
1	120 x 176	120 x 176	120 x 176
2	60 x 88	60 x 88	60 x 88
3	30 x 44	30 x 44	30 x 44
4	15 x 22	15 x 22	15 x 22

Table 5: Size of wavelet decomposed watermark components

Level	Horizontal	Vertical	Diagonal
1	8 x 8	8 x 8	8 x 8

We embedded the first level transformed watermark components to the multilevel transformed components using the watermarking scheme described in Section 2. Selected host and marked video frames are shown in Fig. 12, where we did not notice any artifact or hindrance caused by the watermark. On playing both of the host and marked video using an MPEG video player we also did not notice any obstruction inflicted by the embedded watermark.

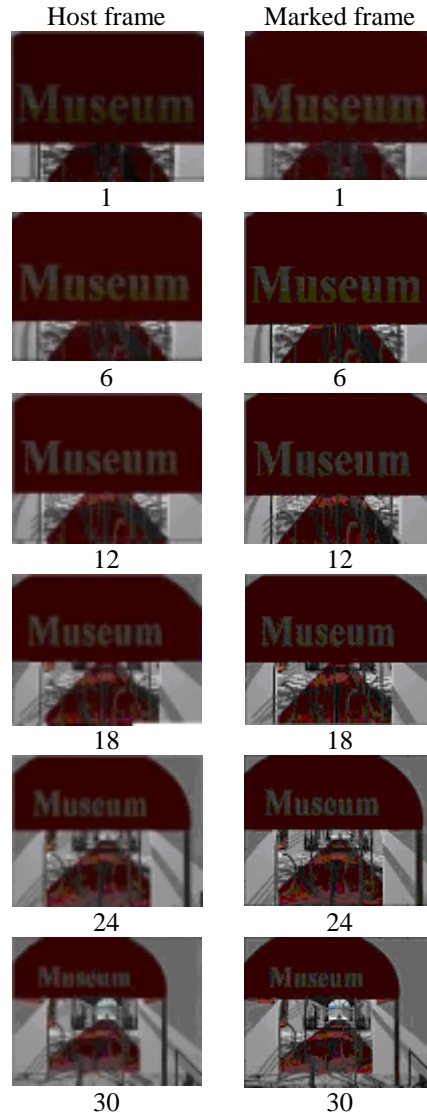


Fig. 12: Marked movie frames

We successfully extracted the watermark using the scheme provided in Section 2. As an example, original and extracted watermarks from frame No. 1 is show in Fig. 13 where we notice high correlation between the original and extracted watermarks that indicates that the presented watermarking scheme has catered for the Guassian noise degradation of the given intensity.

5.1 Effect of Gaussian Noise

For adding the Gaussian noise to the marked images we fixed the mean at zero and changed the variance. We calculated the correlation coefficients, ρ , for the extracted *random* watermark at different SNR values as shown in Fig. 14. We notice that ρ remain above 0.88 in most of the cases and then reach the value 1 for SNR 6.5 dB and above. The correlation coefficients are well above the set criteria, which indicate that our method sustained the degradation caused by the Gaussian noise of the selected variance.

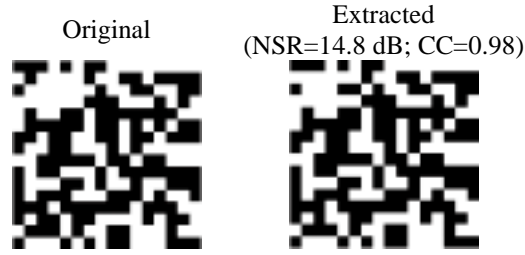


Fig. 13: Original and extracted *random* watermarks

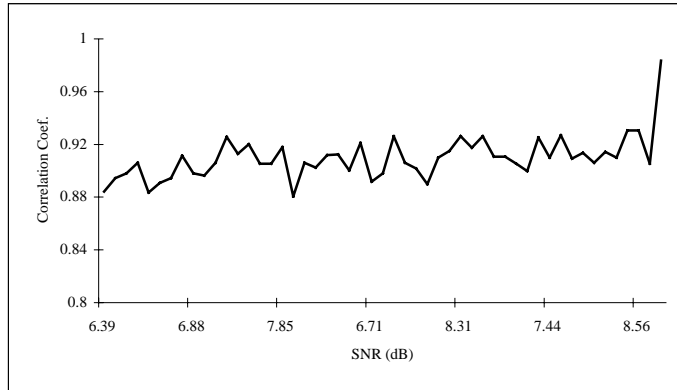


Fig. 14: Result for additive *Gaussian* noise

5.2 Effect of Salt and Pepper Noise

The random salt and pepper noise of various densities was added to the marked image. Fig. 15 show the correlation coefficient, ρ , patterns at different SNR values for the extracted *random* watermark *salt and pepper* noised frame. For the selected range of noise the ρ started increasing from 0.5 and reached its maximum value 1 gradually. The correlation coefficient criteria of 0.75 is achieved at about 3 dB which is an acceptable value.

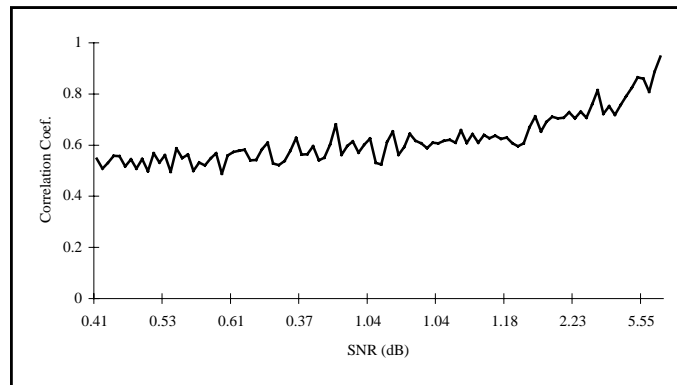


Fig. 15: Result for additive *salt and pepper* noise

5.3 Effect of Speckle noise

Next the marked images were distorted by random Speckle noise of different density values. Fig. 16 show the correlation coefficients, ρ , patterns at different SNRs for the extracted watermarks from *Speckle* noised marked frame. The correlation coefficient crosses the value of 0.75 at about 2.5 dB and then increases to 1 gradually.

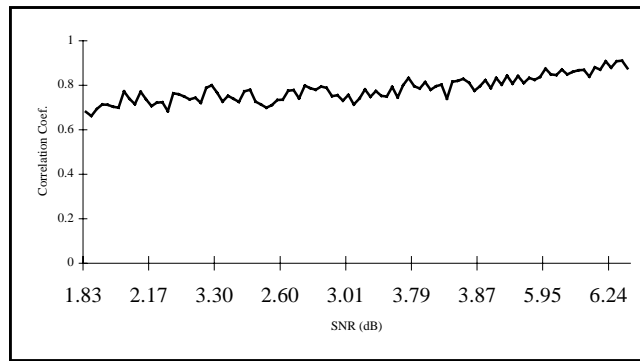


Fig. 16: Result for additive Speckle noise

6.0 CONCLUSION

We employed a watermarking method using discrete wavelet transformation and used a *random* and a *text* watermark for testing. The watermarks thus embedded were found perceptually non-obstructive on six different gray level images and a mpeg color video. The performance of our method was compared with an earlier work and was found better. We tested the robustness of the proposed method by adding four standard noises to the marked images.

For all gray scale images the watermarks were extracted from noisy images to an acceptable degree of correlation. Highest correlation was achieved for the tyre image and result was consistent with all four noises. In comparing the noises, highest correlation coefficient, ρ , is obtained for the case of Gaussian noise with ρ above 0.96 in most cases and with irregularities in the distribution at smaller SNR of less than 47.0 dB. For SNR greater than 50.0 dB, there is not much variation in ρ for all images. The shape of the distribution is more regular for other noises at all values of SNR with ρ above 0.5. For the JPEG noise, at each SNR value, there is not much variation in ρ for all images. For the case of salt and pepper and Speckle noises, there is a variation of ρ for different images at each SNR but ρ distribution follows the same shape.

We also tested the described watermarking method with a mpeg color video comprised of 30 frames. The watermarks embedded using presented scheme were found to be imperceptible on visual inspection of individual frames and video. The marked images were also subjected to *Gaussian*, *salt and pepper* and *Speckle* noises. The watermark was successfully extracted from noisy image to an acceptable degree of correlation.

Therefore we can safely say that in case of gray scale images the proposed method has coped with the additive *Gaussian*, *salt and pepper*, *Speckle*, and *JPEG* noises of different intensity for the selected host images and random and text watermarks. And the described method has also sustained the degradation caused by *Gaussian*, *salt and pepper*, and *Speckle* noises of the adopted range on mpeg color video using random watermark.

REFERENCES

- [1] C. T. Hsu and J. L. Wu, "Hidden Digital Watermarks in Images". *IEEE Trans. on Image Processing*, Vol. 8, No. 1, Jan. 1999, pp. 58-68.
- [2] N. Memon and P. W. Wong, "Protecting Digital Media Content". *Communications of the ACM*, Vol. 41, July 1998, pp. 35-43.
- [3] F. A. P. Petitcolas, R. J. Anderson, and M. G. Kuhn, "Information Hiding - A Survey", in *Proc. of the IEEE - Special Issue on Identification and Protection of Multimedia Information*, July 1999, pp. 1062-1078.
- [4] F. Hartung and M. Kutter, "Multimedia Watermarking Techniques", in *Proc. of IEEE - Special Issue on Identification and Protection of Multimedia Information*, July 1999, pp. 1079-1107.

- [5] I. J. Cox, J. Killian, T. Leighton, and T. Hamoon, "Secure Spread Spectrum Watermarking for Multimedia". *Tech. Rep. 95-10*, NEC Research Institute, 1995.
- [6] J. Ohnishi and K. Matsui, "Embedding a Seal into a Picture Under Orthogonal Wavelet Transform", in *Proc. Int. Conf. on Multimedia Computing and Systems*, June 1996, pp. 514-521.
- [7] D. Kundur and D. Hatzinakos, "A Robust Digital Image Watermarking Method Using Wavelet-Based Fusion", in *Proc. of IEEE Int. Conf. on Acoustics, Speech and Signal Processing*, Seattle, Washington, Vol. 5, May 1997, pp. 544-547.
- [8] A. G. Bors and I. Pitas, "Image Watermarking Using DCT Domain Constraints", in *Proc. IEEE Int. Conf. on Image Processing*, Vol. 3, 1996, pp. 231-234.
- [9] R. G. Van Schyndel, A. Z. Tirkel, and C. F. Osborne, "A Digital Watermark", in *Proc. of Int. Conf. in Image Processing*, Vol. 2, 1994, pp. 86-90.
- [10] D. Kundur and D. Hatzinakos, "Digital Watermarking Using Multiresolution Wavelet Decomposition", in *Proc. of IEEE Int. Conf. on Acoustics, Speech and Sig. Processing*, Seattle, Washington, Vol. 5, May 1998, pp. 2969-2972.
- [11] M. S. Shaikh and Y. Dote, "A Robust Watermarking Method for Copyright Protection of Digital Images Using Wavelet Transformation". *IEEJ Trans. EIS*, Vol. 123, No. 2, 2003, pp. 262-266.
- [12] M. S. Shaikh and Y. Dote, "A Robust Multilevel Watermarking Method for Digital Images Using Multiresolution Wavelet Decomposition", in *Proc. of 6th Online World Conf. on Soft Computing in Industrial Applications (WSC6)*, (<http://vision.fhg.de/wsc6/>), Sept. 10-24, 2001.
- [13] C. C. Wah, "Novel Approach in Watermarking of Digital Image", in *Proc. of Int. Workshop on Soft Computing in Industry'99 (IWSCI'99)*, Muroran, Japan, June 16-18, 1999, pp. 224-227.
- [14] C.-T. Hsu and J.-L. Wu, "Digital Watermarking for Video", in *Proc. of 13th Int. Conf on Digital Signal Processing*, 1997, pp. 217-220.
- [15] J. Dittmann, M. Stabenau, and R. Steinmetz, "Robust MPEG Video Watermarking Technologies". *Report available at <http://www.ipsi.fhg.de/mobile/publications/fullpapers/ACM/index.htm>*.

BIOGRAPHY

Muhammad Shafique Shaikh was born in 1961 in Hyderabad, Pakistan. He received B.Sc. and M. Sc. degrees in Electronics and Computer Technology from University of Sind, Pakistan, in 1983 and 1984, respectively. From 1985 to 1995 he worked in a Pakistan's space agency. He completed his M.Eng. in Computer Science and Systems Engineering at Muroran Institute Technology, Muroran, Japan, in 1999. Currently, Shaikh is a D. Eng. candidate at the same institute. His research interests include signal and image processing, neural networks and watermarking for digital images and videos.

Yasuhiko Dote was born in Sappora, Japan, in 1941. He received his BS degree from Muroran Institute of Technology, Muroran, Japan, in 1963. He completed the M.S. and Ph.D. at University of Missouri, Columbia, in 1972 and 1974, respectively. From 1963 to 1973, he has worked in Yaskawa Electric Manufacturing Co. Ltd., Japan. Presently, Dr. Dote is a Professor in Division of Computer Science and Systems Engineering, Muroran Institute of Technology, Japan. He has many research papers to his credit and has authored and co-authored three books. He has also organised/chaired many national and international conferences. His research interests include intelligent control, soft computing and power electronics.